

# Tree species and age class mapping in a Central European woodland using optical remote sensing imagery and orthophoto derived stem density – Performance of multispectral and hyperspectral sensors

M. Schlerf, C. Atzberger & J. Hill

*Remote Sensing Department, University of Trier, Geozentrum, D-54286 Trier, Germany*

**Keywords:** forestry, hyperspectral, classification

**ABSTRACT:** Optical remote sensing imagery and orthophoto derived stem density were classified to map coniferous forest cover for a study area located in the Western Hunsrück, Germany. Our objectives were (i) to investigate if hyperspectral data contain more information relevant to classification of species and age classes than multispectral imagery and (ii) to test in what way classification results can be improved through the integration of orthophoto derived stem densities into the classification process.

Airborne hyperspectral data (HyMap) covering the entire test site has been acquired for July 1999. Subsequent to radiometric and geometric correction, data reduction and enhancement was performed by a Minimum Noise Fraction transformation. Multispectral data (TM) was simulated through degradation of the spectral and/or spatial information of the HyMap data. Three different synthetic datasets were created: spectrally degraded, spatially degraded and a combination of both. Stem density information were added to the original HyMap imagery for classification purpose. Stem density had previously been derived from black/white orthophotos by an automatic method. Classification was achieved by the Spectral Angle Mapper algorithm.

Our results show that mapping of coniferous forest cover is improved by the use of hyperspectral imagery compared to multispectral data and that classification accuracy is greater using 30 m spatial resolution data compared to 5 m resolution data. Integration of orthophoto derived stem density into the classification process resulted in slightly better performance compared to the results obtained with image data alone.

## 1 INTRODUCTION

Knowledge about forest species and age is critical to both forest resource management and scientific research. For instance, forest inventories routinely collect species distribution in forest stands and timber volume estimates highly depend on stand age. Biogeochemical process models, such as Forest-BGC (Running & Coughlan, 1988; Running, 1994) parameterize certain model input variables depending on tree species.

Forest species and age recognition can, apart from field survey, reliably achieved through aerial photo interpretation. Data from broad band remote sensing instruments have been used to distinguish between coniferous and deciduous stands (Nelson et al., 1985) and at more detailed species resolution (Franklin, 1994; Vohland, 1997). Detailed mapping of forest species and age classes through remote sensing can either be improved by high spatial or high spectral resolution sensors.

Use of hyperspectral data for forest studies has mainly been focused on biochemistry (Peterson et al., 1988; Wessman et al., 1988; Johnson et al.,

1994; Gastellu-Etchegorry et al., 1995) and leaf area index (Gong et al., 1992). However, few studies have reported on the use of hyperspectral data in mapping forest species. In situ hyperspectral data has been explored to discriminate six conifer species (Gong et al., 1997) and several tropical species (Cochrane, 2000). Hyperspectral image data has been used for differentiation of forest species (Franklin, 1994; Martin et al., 1998) and for algal species recognition (Alberotanza et al., 1999). Even less studies have been carried out to identify forest age classes from hyperspectral imagery.

## 2 OBJECTIVES

The objectives of this study were (i) to compare the classification performance of four different remote sensing datasets with different spectral and spatial resolution to map forest species and age classes and (ii) to investigate if additional information on stem density can improve the classification results. Three

hypotheses associated with the objectives have been formulated:

Hypothesis 1: An increase in image variance due to higher spatial resolution might lead to problems in the classification process. This assumption is supported by classification results obtained by Martin & Howarth (1989) who found that an increase in spatial resolution did not result in higher classification accuracies. In the case of forest cover, each tree crown which is distinguishable in the high resolution imagery will have a sunlit and shaded portion with a highly variable spectral response. Moreover, relatively small gaps in the forest cover where under story vegetation or bare soil become visible might be resolved in the image. These effects are largely smoothed out in the low resolution dataset with the effect of a lower spatial variance. Thus, we expect a better classification result from the dataset with 30 m compared to the one with 5 m resolution.

Hypothesis 2: As hyperspectral data probably contain more information relevant to the classification of forest cover than broadband multispectral data, we expect a better performance of the high spectral resolution imagery in terms of classification accuracy. Contrary to broad band data analysis techniques, hyperspectral data offer the use of full-spectrum analysis techniques that exploit all the inherent information. As an example, it has already been shown that the estimation of canopy LAI using hyperspectral imagery can be achieved with an accuracy greater than would be expected with a broadband sensor (Gong et al, 1992).

Hypothesis 3: The results of the classification of forest cover may be improved through addition of orthophoto derived stem densities into the classification process. Various other types of ancillary information have already been utilized in multispectral classification of vegetation cover: Wulder (1998), for instance, used texture and Franklin (1994) used digital elevation models as additional information and observed an increase of overall classification accuracy compared to using remote sensing data on a pixel basis alone.

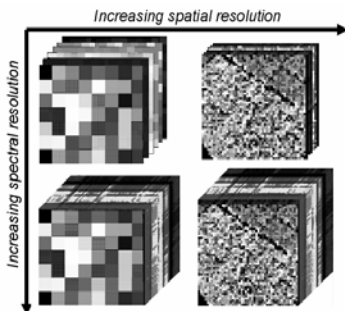


Figure 1. Four datasets of varying spectral and spatial resolution. Upper left: TM, 30 m; upper right: TM, 5 m; lower left: HyMap, 30 m; lower right: HyMap, 5 m.

### 3 STUDY AREA AND DATA

The area of study (49°40'N, 7°10'E) is located in the Idarwald forest in south-western Germany on the north-western slope of the Hunsrück mountain ridge. The dominant forest species are Norway spruce (*picea abies*), beech (*fagus sylvatica*), oak (*quercus petraea*) and Douglas fir (*pseudotsuga menziesii*). Active forestry practices in this area include selective cutting, plantation establishment and thinning.

Hyperspectral image data were acquired using the HyMap sensor built by Integrated Spectronics, Australia in July 1999. HyMap records data in 128 contiguous spectral bands covering the spectral range of 0.4-2.5  $\mu\text{m}$  with a spectral resolution of 10-20 nm. The spatial resolution was set to 5 m with a full scene covering 4 km x 10 km.

Radiometric corrections of the HyMap data were performed at the Remote Sensing Department, University of Trier following an approach by Hill et al. (1995, 2001). The processing steps involved atmospheric correction and sensor calibration. The first step converted digital numbers to at-sensor-radiances. In the second step, the effects of the atmosphere were removed including errors due to pixel orientation. The dataset was geocoded using parametric image processing software PARGE (Schläpfer et al., 1998)

The most recent forest inventory for the study area (01.10.1994) including stand information on species composition and age classes has been integrated into a Geographical Information System (FoGIS) by Vohland (1997).

Stem density had previously been estimated from aerial orthophotos by automatic identification and counting of individual tree crowns (Atzberger & Schlerf, 2002a; b). Stem density was integrated into the FoGIS and mean as well as standard deviation at forest stand level were calculated.

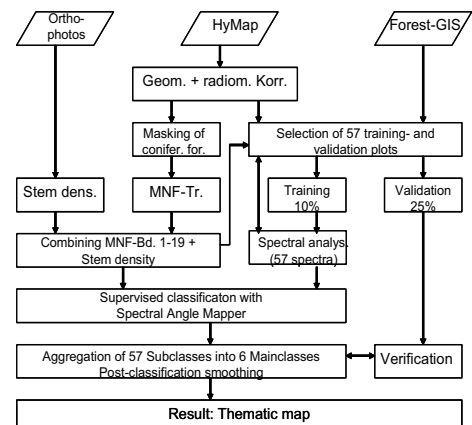


Figure 2. Data input and processing steps followed for the classification of forest cover.

#### 4 METHODS

The classification was carried out for each of the four datasets separately (Figure 1). Stem density was solely added to the dataset with high spectral and high spatial resolution. The procedure used for the classification of the conifer forest cover using the high spectral resolution dataset in combination with the stem density was as follows (Figure 2):

- Masking of the deciduous forest cover for separation from the coniferous stands. The mask was generated through an unsupervised classification of the HyMap data (Isodata algorithm).
- Data reduction and enhancement of the hyperspectral data was performed by a Minimum Noise Fraction transformation (Green et al., 1988; Lee et al. 1990). The first 19 MNF-fractions were separated from the remaining fractions and used for further analysis. Synthetic TM-datasets were created by selecting those HyMap bands that correspond to the central wavelengths of the broad Thematic Mapper bands. Spatial degradation of the high spatial resolution data (5 m) was done by calculating the mean pixel value within a 30 m x 30 m array.
- The aim of the training stage is to collect a set of statistics that describe the spectral response pattern for each species/age class. The polygons in the FoGIS representing the forest stands were used to extract spectral signatures for each class (5-15 polygons per class, 100-1000 pixels per polygon). In total, 57 subclasses and 52.844 pixels were obtained. Training data were divided randomly into three sets of pixels: 10 percent were used for training (training pixels), 25 percent for validation of the classification result (validation pixels) and the remaining 65 percent pixels were not used. The training setup was designed this way to reflect the small amount of ground truth commonly available in reality. After a visual interpretation of the collected spectra (Figure 3) it was decided to chose 6 species/age classes for classification (Norway spruce: 4 age classes; Douglas fir: 2 age classes).
- The Spectral Angle Mapper (Kruse et al, 1993) was employed for supervised classification. The algorithm determines the spectral similarity between two spectra by calculating the angle between the spectra, treating them as vectors in a space with dimensionality equal to the number of bands (Kruse et al, 1993). SAM compares the angle between the spectrum vector of the known class and each pixel vector (unknown class) in n-dimensional space. In the classification stage, the class with the smallest angle is assigned to the corresponding image pixel.
- The 57 subclasses obtained from the classification were condensed into the 6 main classes. Then post-classification smoothing was per-

formed to remove single isolated image pixels (sieve and clump).

- To assess the accuracy the validation pixels were used. A confusion matrix was generated from the validation pixels for each classification. Two measures of classification accuracy are reported. Overall accuracy (OAA) quantifies the percentage of cases correctly classified:

$$OAA = \frac{\sum_{k=1}^q n_{kk}}{n} * 100 \quad (1)$$

where  $n_{kk}$  is the number of correctly classified validation pixels (confusion matrix diagonals),  $q$  is the number of classes, and  $n$  is the total number of validation pixels used.

The kappa coefficient accommodates for the effects of chance agreement:

$$KAPPA = \frac{n \sum_{k=1}^q n_{kk} - \sum_{k=1}^q n_{k+} n_{+k}}{n^2 - \sum_{k=1}^q n_{k+} n_{+k}} \quad (2)$$

where  $n_{k+}$  is the sum of the validation pixels in a class and  $n_{+k}$  is the sum of the classified pixels in that class.

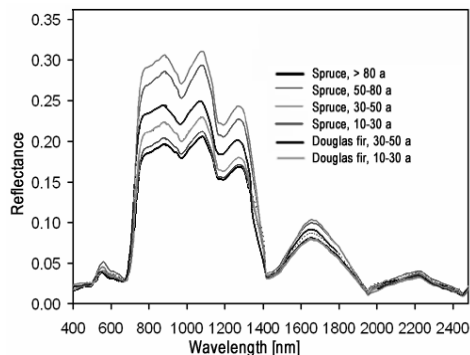


Figure 3. Reflectance spectra of Norway spruce and Douglas fir of different age.

#### 5 RESULTS AND DISCUSSION

Table 1 lists confusion matrices obtained from classifying each of the 5 sets of data (2 types of spectral resolution x 2 types of spatial resolution plus 1 type high spectra and high spatial resolution combined with stem density). Table 2 lists overall accuracies and kappa coefficients for the same datasets.

Table 1. Confusion matrices for 5 different datasets: A: hyperspectral, 5 m; B: hyperspectral, 30 m; C: multispectral, 5 m; D: multispectral 30 m, E: hyperspectral 5 m and orthophoto derived stem density

A)

| Class        | Ground Truth (Percent) |             |             |             |             |             | Total |
|--------------|------------------------|-------------|-------------|-------------|-------------|-------------|-------|
|              | Spr. >80a              | Spr. 50-80a | Spr. 30-50a | Spr. 10-30a | Dou. 30-50a | Dou. 10-30a |       |
| Unclassified | 4.2                    | 4.1         | 8.1         | 1.2         | 2.8         | 1.7         | 4.4   |
| Spr. >80a    | 84.1                   | 6.8         | 3.8         | 0.2         | 0.1         | 0.0         | 16.4  |
| Spr. 50-80a  | 10.3                   | 86.7        | 29.2        | 0.0         | 3.8         | 0.2         | 32.6  |
| Spr. 30-50a  | 1.1                    | 2.2         | 58.1        | 0.7         | 2.0         | 0.4         | 15.1  |
| Spr. 10-30a  | 0.3                    | 0.2         | 0.6         | 97.9        | 1.0         | 2.4         | 9.1   |
| Dou. 30-50a  | 0.0                    | 0.0         | 0.1         | 0.0         | 89.5        | 0.8         | 14.5  |
| Dou. 10-30a  | 0.0                    | 0.0         | 0.0         | 0.0         | 0.7         | 94.5        | 7.8   |
|              | 100.0                  | 100.0       | 100.0       | 100.0       | 100.0       | 100.0       | 100.0 |

B)

| Class        | Ground Truth (Percent) |             |             |             |             |             | Total |
|--------------|------------------------|-------------|-------------|-------------|-------------|-------------|-------|
|              | Spr. >80a              | Spr. 50-80a | Spr. 30-50a | Spr. 10-30a | Dou. 30-50a | Dou. 10-30a |       |
| Unclassified | 2.8                    | 3.9         | 1.3         | 3.0         | 1.1         | 2.2         | 2.4   |
| Spr. >80a    | 95.4                   | 0.0         | 0.1         | 0.0         | 0.0         | 1.8         | 17.7  |
| Spr. 50-80a  | 1.6                    | 92.3        | 4.5         | 0.0         | 0.0         | 0.0         | 25.5  |
| Spr. 30-50a  | 0.2                    | 3.7         | 94.0        | 0.0         | 0.1         | 0.0         | 22.6  |
| Spr. 10-30a  | 0.0                    | 0.0         | 0.0         | 97.0        | 0.0         | 0.1         | 6.2   |
| Dou. 30-50a  | 0.0                    | 0.0         | 0.0         | 0.0         | 98.8        | 0.0         | 15.9  |
| Dou. 10-30a  | 0.0                    | 0.0         | 0.0         | 0.0         | 0.0         | 95.9        | 9.6   |
| Total        | 100.0                  | 100.0       | 100.0       | 100.0       | 100.0       | 100.0       | 100.0 |

C)

| Class        | Ground Truth (Percent) |             |             |             |             |             | Total |
|--------------|------------------------|-------------|-------------|-------------|-------------|-------------|-------|
|              | Spr. >80a              | Spr. 50-80a | Spr. 30-50a | Spr. 10-30a | Dou. 30-50a | Dou. 10-30a |       |
| Unclassified | 3.7                    | 1.8         | 7.0         | 0.6         | 20.0        | 4.4         | 6.5   |
| Spr. >80a    | 32.1                   | 15.1        | 2.3         | 0.0         | 0.5         | 0.0         | 10.4  |
| Spr. 50-80a  | 63.3                   | 81.6        | 48.3        | 0.0         | 22.0        | 0.4         | 47.6  |
| Spr. 30-50a  | 0.0                    | 0.1         | 38.3        | 14.3        | 3.8         | 0.6         | 10.4  |
| Spr. 10-30a  | 1.0                    | 1.3         | 4.0         | 84.2        | 0.6         | 4.9         | 7.4   |
| Dou. 30-50a  | 0.0                    | 0.0         | 0.0         | 0.0         | 46.7        | 20.3        | 9.5   |
| Dou. 10-30a  | 0.0                    | 0.0         | 0.2         | 1.0         | 6.4         | 69.4        | 8.1   |
| Total        | 100.0                  | 100.0       | 100.0       | 100.0       | 100.0       | 100.0       | 100.0 |

D)

| Class        | Ground Truth (Percent) |             |             |             |             |             | Total |
|--------------|------------------------|-------------|-------------|-------------|-------------|-------------|-------|
|              | Spr. >80a              | Spr. 50-80a | Spr. 30-50a | Spr. 10-30a | Dou. 30-50a | Dou. 10-30a |       |
| Unclassified | 8.0                    | 6.4         | 10.8        | 17.8        | 4.8         | 3.3         | 7.9   |
| Spr. >80a    | 44.1                   | 10.6        | 1.1         | 0.0         | 0.0         | 0.5         | 11.2  |
| Spr. 50-80a  | 41.9                   | 83.0        | 41.1        | 0.0         | 0.0         | 0.0         | 38.9  |
| Spr. 30-50a  | 6.0                    | 0.0         | 45.7        | 5.0         | 0.0         | 0.0         | 11.9  |
| Spr. 10-30a  | 0.0                    | 0.0         | 1.3         | 77.2        | 0.2         | 3.2         | 5.6   |
| Dou. 30-50a  | 0.0                    | 0.0         | 0.0         | 0.0         | 94.3        | 2.3         | 15.4  |
| Dou. 10-30a  | 0.0                    | 0.0         | 0.0         | 0.0         | 0.7         | 90.8        | 9.2   |
| Total        | 100.0                  | 100.0       | 100.0       | 100.0       | 100.0       | 100.0       | 100.0 |

E)

| Class        | Ground Truth (Percent) |             |             |             |             |             | Total |
|--------------|------------------------|-------------|-------------|-------------|-------------|-------------|-------|
|              | Spr. >80a              | Spr. 50-80a | Spr. 30-50a | Spr. 10-30a | Dou. 30-50a | Dou. 10-30a |       |
| Unclassified | 3.5                    | 3.6         | 5.5         | 0.5         | 2.1         | 1.5         | 3.3   |
| Spr. >80a    | 90.0                   | 10.3        | 4.1         | 0.0         | 0.4         | 0.0         | 18.4  |
| Spr. 50-80a  | 5.6                    | 84.3        | 25.4        | 0.1         | 3.4         | 0.1         | 30.2  |
| Spr. 30-50a  | 0.6                    | 1.7         | 64.3        | 0.1         | 2.8         | 0.4         | 16.5  |
| Spr. 10-30a  | 0.4                    | 0.1         | 0.6         | 99.3        | 0.5         | 2.4         | 9.1   |
| Dou. 30-50a  | 0.0                    | 0.0         | 0.1         | 0.0         | 89.9        | 0.7         | 14.6  |
| Dou. 10-30a  | 0.0                    | 0.0         | 0.1         | 0.0         | 0.9         | 94.9        | 7.9   |
| Total        | 100.0                  | 100.0       | 100.0       | 100.0       | 100.0       | 100.0       | 100.0 |

Table 2. Summary of accuracies.

| Dataset                     | Overall Accuracy | Kappa Coefficient |
|-----------------------------|------------------|-------------------|
| A: HyMap 5m                 | 81.4             | 0.78              |
| B: HyMap 30m                | 95.0             | 0.94              |
| C: TM 5 m                   | 55.9             | 0.47              |
| D: TM 30 m                  | 69.5             | 0.64              |
| E: HyMap 5 m + Stem density | 83.5             | 0.81              |

The overall accuracy (OAA) using the dataset A (HyMap, 5 m) was 81 percent. This increased to 95 percent using HyMap degraded to 30 m spatial resolution (dataset B). Essentially the same tendency was obtained in classifying TM 5 m (dataset C) and TM 30 m (dataset D). OAA using TM datasets were generally considerably lower than those of HyMap datasets.

The OAA using the full set of HyMap 5 m data and stem density information (dataset E) was 83 percent and thus 2 percent greater than the OAA using HyMap 5 m (dataset A) alone.

The obtained results clearly confirm hypotheses 1 and 2. Concerning hypothesis 3, it can not definitely be concluded that stem density information is critical for the classification of species/age classes. To further investigate this problem, stem density should also be added to the other datasets in the classification process.

## 6 CONCLUSIONS AND FUTURE TASKS

The potential of various sensors in recognition of forest cover is not yet fully identified. Current and future developments in sensor design are heading towards an increase in spatial and/or spectral resolution. From this study, it can be concluded that classification accuracies benefit from an increase in spectral resolution. On the other hand, an increase in spatial resolution does not yield better classification results of conifer species and age when performed on pixel basis. However, no use was made of the information inherent in the high spatial resolution imagery concerning texture.

Future tasks to be implemented into forest cover classification of hyperspectral imagery comprise spectral derivatives and neural network classifier which have already been tested with success on *in situ* data by Gong et al. (1997, 2001). In addition, the extent of improving the classification should be determined for various types of texture measures.

## ACKNOWLEDGMENTS

This research was financially supported by the German Research Community (DFG). The authors are grateful to Dr. Patrick Hostert, Dr. Thomas Udelhoven, Wolfgang Mehl (Joint Research Centre, Ispra, Italy), Samuel Bärtsch and Sebastian Mader who were involved into the pre-processing of the HyMap data. The Forest-GIS was provided by Michael Vohland and is gratefully acknowledged. Thanks are also expressed to Dr. Patrick Hostert for offering suggestions which improved the concept of the classification procedure. The over-flight with the HyMap-sensor was organized by Andreas Müller and

Andrea Haushold of the German Aerospace Center (DLR).

## REFERENCES

- Alberotanza, L.; Brando, V.E.; Ravagnan, G.; Zandonella, A. (1999): Hyperspectral aerial images. A valuable tool for submerged vegetation recognition in the Orbetello lagoons, Italy. *Remote Sens. Environ.*, 3: 523-533.
- Atzberger, C. & Schlerf, M. (2002a): Automatisierte Bestimmung der Bestockungsdichte in Nadelwäldern aus räumlich hochauflösenden Orthofotobildern. *Photogrammetrie, Fernerkundung, Geoinformation* (in press).
- Atzberger, C. & Schlerf, M. (2002b): Object-based stem density estimates in a mid-European forest district based on artificial neural nets – Comparison of Landsat-TM and HyMAP performances. In: *Proc. of the 22<sup>nd</sup> EARSeL Symposium "Geoinformation for European-wide integration"*, 4-6 June 2002, Prague (this issue).
- Cochrane, M. A. (2000): Using vegetation reflectance variability for species level classification of hyperspectral data. *Int. Jour. Rem. Sens.*, 10: 2075-2087.
- Foody, G.M. (2002): Status of land cover classification accuracy assessment. *Remote Sens. Environ.*, 80: 185-201.
- Franklin, S. E. (1994): Discrimination of subalpine forest species and canopy density using digital CASI, SPOT PLA, and Landsat TM data. *Photogr. Eng. & Rem. Sens.*, 60(10): 1233-1241.
- Gastellu-Etcheberry, J. P.; Zagolski, F.; Mouglin, E.; Marty, G.; Giordano, G. (1995): An assessment of canopy chemistry with AVIRIS - a case study in the Landes Forest, Southwest France. *Int. Jour. Rem. Sens.*, 16 (3): 487-501.
- Gong, P.; Pu, R.; Miller, J.R. (1992): Correlating leaf area index of Ponderosa pine with hyperspectral CASI data. *Canadian Journal of Remote Sensing*, 18: 275-282.
- Gong, P.; Pu, R.; Yu, B. (1997): Conifer species recognition: an exploratory analysis of *in situ* hyperspectral data. *Remote Sens. Environ.*, 62: 189-200.
- Gong, P.; Pu, R.; Yu, B. (2001): Conifer species recognition: effects of data transformation. *Int. Jour. Rem. Sens.*, 17: 3471-3481.
- Green, A. A.; Berman, M.; Switzer, P.; Craig, M. D. (1988): A transformation for ordering multispectral data in terms of image quality with implications for noise removal. *IEEE Trans. Geosc. Rem. Sens.*, 26, 1: 65-74.
- Hill, J. (2001): Sensorkalibration und atmosphärische Korrektur von hyperspektralen Fernerkundungsdaten. In: *Müller, P. et al. (Eds.): Umwelt und Region – aus der Werkstatt des Sonderforschungsbereiches 522*, Trier, Selbstverlag: 175-182.
- Hill, J.; Mehl, W.; Radeloff, V. (1995): Improved forest mapping by combining corrections of atmospheric and topographic effects. In: *J. Askne (Ed.): Sensors and environmental applications of remote sensing, Proc. 14th EARSeL Symposium, Göteborg, Sweden, 6-8 June 1994*. A.A. Balkema: Rotterdam, Brookfield: 143-151.
- Johnson, L. F.; Hlavka, C. A.; Peterson, D. L. (1994): Multivariate analysis of AVIRIS data for canopy biochemical estimation along the Oregon transect. *Remote Sens. Environ.*, 47: 216-230.
- Kruse, F. A.; Lefkoff, A. B.; Boardman, J. B.; Heidebrecht, K. B.; Shapiro, A. T.; Barloon, P. J.; Goetz, A. F. H. (1993): The spectral image processing system (SIPS) -Interactive visualization and analysis of imaging spectrometer data. *Remote Sens. Environ.*, 44: 145-163.
- Lee, J. B., Woodyatt, A. S., and Berman, M. (1990): Enhancement of high spectral resolution remote sensing data by

- noise-adjusted principal components transform. *IEEE Trans. Geosc. Rem. Sens.* 28, 3: 295-304.
- Martin, L.; Howarth, P. (1989): Change-detection accuracy assessment using SPOT multispectral imagery of the rural-urban fringe. *Remote Sens. Environ.*, 30: 55-66.
- Martin, M. E.; Newman, S. D.; Aber, J. D.; Congalton, R. G. (1998): Determining forest species composition using high spectral resolution remote sensing data. *Remote Sens. Environ.*, 65: 249-254.
- Nelson, R. F.; Latty, R. S.; Mott, G. (1985): Classifying northern forests using Thematic Mapper Simulator data. *Photogr. Eng. & Rem. Sens.*, 50: 607-617.
- Peterson, D. L.; Aber, J. D.; Matson, P. A.; Card, D. H.; Swanberg, N.; Wessman, C.; Spanner, M. (1988): Remote sensing of forest canopy and leaf biochemical contents. *Remote Sens. Environ.*, 24: 85-108.
- Running, S. W. (1994): Testing Forest-BGC ecosystem process simulations across a climatic gradient in Oregon. *Ecol. Appl.*, 4: 238-247.
- Running, S. W. & Coughlan, J. C. (1988): A general model for forest ecosystem processes for regional applications. I. Hydrologic balance, canopy gas exchanges and primary production processes. *Ecol. Model.* 42: 125-154.
- Schläpfer D.; Schaepman M. E.; Itten K. I. (1998): PARGE: Parametric Geocoding Based on GCP- Calibrated Auxiliary Data. *SPIE Int. Symp. on Opt. Sc, Eng. and Instr.*, San Diego (CA): 334-344.
- Vohland, M. (1997): Einsatz von Satellitenbilddaten (Landsat TM) zur Ableitung forstlicher Bestandsparameter und Waldschadensindikatoren. Diplomarbeit, Universität Trier.
- Wessman, C. A.; Aber, J. D.; Peterson, D. L.; Melillo, J. M. (1988): Remote sensing of canopy chemistry and nitrogen cycling in temperate forest ecosystems. *Nature*, 335: 154-156.
- Wulder, M. (1998): Optical remote-sensing techniques for the assessment of forest inventory and biophysical parameters. *Progr. Phys. Geogr.*, 22(4): 449-476.